

# Suzaku Observation of Six New *Swift*/BAT AGNs: Evidence for Two Types of Obscured Population

Satoshi Eguchi<sup>1</sup>, Yoshihiro Ueda<sup>1</sup>, Yuichi Terashima<sup>2</sup>, Richard Mushotzky<sup>3</sup> and Jack Tueller<sup>3</sup>

<sup>1</sup> Department of Astronomy, Kyoto University, Kyoto 606-8502, Japan

<sup>2</sup> Department of Physics, Faculty of Science, Ehime University, Matsuyama 790-8577, Japan

<sup>3</sup> NASA/Goddard Space Flight Center, Greenbelt, MD 20771, USA

*E-mail(SE): eguchi@kusastro.kyoto-u.ac.jp*

## ABSTRACT

We present a systematic spectral analysis with *Suzaku* of six AGNs detected in the *Swift*/BAT hard X-ray (15–200 keV) survey. The 0.5–200 keV spectra of these sources can be uniformly fit with a base model consisting of heavily absorbed ( $\log N_{\text{H}} > 23.5 \text{ cm}^{-2}$ ) transmitted components, scattered lights, a reflection component, and an iron-K emission line. There are two distinct groups, three “new type” AGNs (including the two sources reported by Ueda et al. 2007) with an extremely small scattered fraction ( $f_{\text{scat}} < 0.5\%$ ) and strong reflection component ( $R = \Omega/2\pi \gtrsim 0.8$ , where  $\Omega$  is the solid angle of the reflector), and three “classical type” ones with  $f_{\text{scat}} > 0.5\%$  and  $R \lesssim 0.8$ . The spectral parameters suggest that the new type has an optically thick torus for Thomson scattering ( $N_{\text{H}} \sim 10^{25} \text{ cm}^{-2}$ ) with a small opening angle of  $\theta \sim 20^\circ$  viewed in a rather face-on geometry, while the classical type has a thin torus ( $\log N_{\text{H}} \sim 23\text{--}24 \text{ cm}^{-2}$ ) with  $\theta \gtrsim 30^\circ$ . We infer that a significant number of new type AGNs with an edge-on view is missing in the current all-sky hard X-ray surveys.

KEY WORDS: galaxies: active — gamma rays: observations — X-rays: galaxies — X-rays: general

## 1. Introduction

The origin of the cosmic X-ray background (CXB) is the integrated emission from the whole active galactic nuclei (AGNs) in the universe. The peak intensity of the CXB at  $\sim 30 \text{ keV}$  contains significant contribution from “hidden” AGNs, i.e., those subject to absorption with column densities larger than  $10^{23} \text{ cm}^{-2}$ . However, these AGNs have been difficult to be detected in X-ray surveys below 10 keV due to their heavy absorption.

The *Swift*/BAT performed an all-sky surveys at energies above 15 keV, where photoelectric absorption is inefficient (Tueller et al. 2009). It provides us with the least biased AGN sample in the local universe, including heavily obscured ones. In this paper, we present the results of a systematic spectral analysis of six new *Swift*/BAT AGNs observed with *Suzaku* (Table 1). The results of other *Swift* AGNs are reported by Winter et al. (2009) and Tazaki et al. (this conference).

## 2. Analysis and Results

### 2.1. BAT Spectra

Before performing the spectral fit to the *Suzaku* data, we first analyze only the BAT spectra in the 15–200 keV band to constrain the high energy cutoff in the continuum. It is known that the incident photon spectra of

Seyfert galaxies can be approximated by a power law with an exponential cutoff in the form of  $\exp(-E/E_{\text{cut}})$ , representing the temperature of electrons responsible for Compton scattering. The typical value of  $E_{\text{cut}}$  ranges from 100 keV to 500 keV.

Utilizing the *Swift*/BAT spectra above 15 keV, we try to constrain  $E_{\text{cut}}$ . In this stage, we assume the reflection strength ( $R = \Omega/2\pi$ , where  $\Omega$  is the solid angle of the reflector) to be 0 or 2 as the two extreme cases just to evaluate its effect. While it is difficult to constrain the upper limit of  $E_{\text{cut}}$  due to the limited band coverage of the BAT, we find the cutoff energy must be above  $\sim 100 \text{ keV}$  in most cases. In the following analysis, we fix  $E_{\text{cut}}$  at 300 keV.

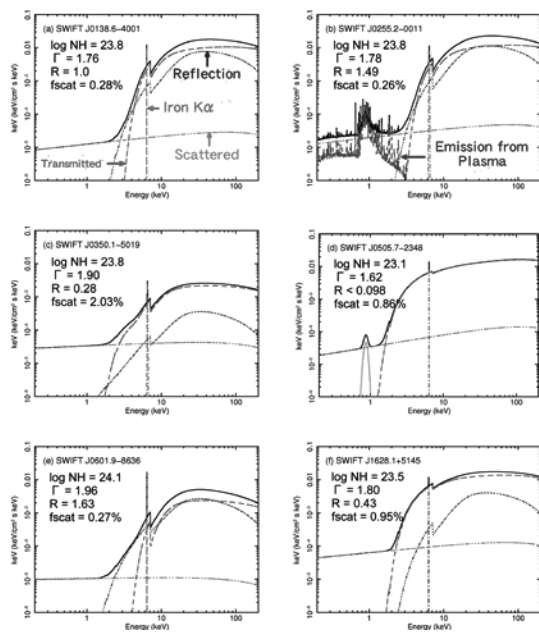
### 2.2. *Suzaku* Spectra

We performed simultaneous fits to the *Suzaku* XIS and HXD/PIN, and the *Swift*/BAT spectra with the following three models:

1. a cutoff power law absorbed by cold matter + a scattered component + an iron-K emission line,
2. a cutoff power law absorbed by cold matter + a scattered component + an iron-K emission line + an absorbed Compton reflection component,

SWIFT	Optical/IR Identification	R.A. (J2000)	Dec. (J2000)	Redshift	Classification
J0138.6–4001	ESO 297–G018	01 38 37.16	-40 00 41.1	0.0252	Seyfert 2
J0255.2–0011	NGC 1142	02 55 12.196	-00 11 0.81	0.0288	Seyfert 2
J0350.1–5019	2MASX J03502377–5018354	03 50 23.77	-50 18 35.7	0.036	Galaxy
J0505.7–2348	2MASX J05054575–2351139	05 05 45.73	-23 51 14.0	0.0350	Seyfert 2
J0601.9–8636	ESO 005–G004	06 05 41.63	-86 37 54.7	0.0062	Galaxy
J1628.1+5145	Mrk 1498	16 28 4.06	+51 46 31.4	0.0547	Seyfert 1.9

Table 1. List of targets. The position, redshift, and classification for each source is taken from the NASA/IPAC Extragalactic Database.

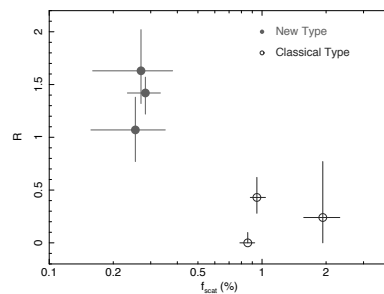
Fig. 1. Best-fit spectral model of the six targets.  $N_{\text{H}}$ ,  $\Gamma$ ,  $R$ , and  $f_{\text{scat}}$  represent the line-of-sight hydrogen column density, the power-law photon index, the intensity of the reflection component relative to the incident power-law component, and the fraction of the scattered component, respectively.

- a cutoff power law absorbed by different two cold matters + a scattered component + an iron-K emission line + an absorbed Compton reflection component.

Based on statistical tests and physical consistency between the equivalent width of the iron-K emission line and the reflection strength, we choose the best model for each targets: SWIFT J0138.6–4001, J0255.2–0011 and J0601.9–8636 are best represented with model 2 and the others are with model 3 (Figure 1).

### 3. Discussion and Conclusion

We find that the absorption column densities of all the targets are larger than  $10^{23.5} \text{ cm}^{-2}$ , i.e., they are “hidden” AGNs. Our *Suzaku* results suggest that there are

Fig. 2. Correlation between the strength of the Compton reflection component ( $R = \Omega/2\pi$ ) and the fraction of the scattered component ( $f_{\text{scat}}$ ) for the six targets.

two groups even within the hidden population (Figure 2), that is, (1)  $R \gtrsim 0.8$  and  $f_{\text{scat}} \lesssim 0.5\%$  (“new type”), and (2)  $R \lesssim 0.8$  and  $f_{\text{scat}} \gtrsim 0.5\%$  (“classical type”). It is notable that  $f_{\text{scat}} < 0.5\%$  is very small when compared with a typical value of 3–10% obtained for optical selected Seyfert 2 samples (e.g., Turner et al. 1997). We can constrain the geometry of the torus from the observed equivalent width of the iron-K emission line and  $f_{\text{scat}}$  value, assuming that the scattering fraction corresponds to the opening angle of the torus. Based on the calculation by Levenson et al. (2002), we estimate that the new type has an optically thick torus ( $\log N_{\text{H}} \sim 25 \text{ cm}^{-2}$ ) with a very small opening angle of  $\theta \sim 20^\circ$  viewed in a rather face-on geometry, while the classical type has a thin torus ( $\log N_{\text{H}} \sim 23\text{--}24 \text{ cm}^{-2}$ ) with  $\theta \gtrsim 30^\circ$  viewed in an edge-on geometry. Finally, we infer that a significant number of new type AGNs with an edge-on view is missing in the current all-sky hard X-ray ( $> 10 \text{ keV}$ ) surveys, requiring even more sensitive observations in hard X-rays to detect them completely.

### References

- Eguchi et al. 2009 ApJ, 696, 1657  
 Levenson et al. 2002 ApJ, 573, L81  
 Tueller et al. 2009 arXiv:0930.3037  
 Turner et al. 1997 ApJS, 113, 23  
 Ueda et al. 2007 ApJ, 664, L79  
 Winter et al. 2009 ApJ, 701, 1644